Pergamon

Polyhedron Vol. 14, No. 19, pp. 2603–2612, 1995
Elsevier Science Ltd
Printed in Great Britain
0277–5387/95 $9.50+0.00

0277–5387(95)00126–3

FLUXIONALITY IN $(BH_4)Mn(CO)_4$ AND $(BH_4)Cu(PH_3)_2$*

YASUO OISHI and THOMAS A. ALBRIGHT†

Department of Chemistry, University of Houston, Houston, Texas 77204-5641, U.S.A.

and

HIROSHI FUJIMOTO

Division of Molecular Engineering, Kyoto University, Kyoto 606, Japan

Abstract—Molecular orbital calculations at the *ab initio* level have been carried out for $(BH_4)Mn(CO)_4$ and $(BH_4)Cu(PH_3)_2$. The geometries were optimized at the η^2 ground states, as well as η^1 and two η^3 structures. Single point calculations at higher levels of theory show that the η^1 structures for both molecules lie at decisively higher relative energies than the η^3 geometries. Thus, the mechanism of bridging–terminal hydride exchange presumably occurs via an associative rather than dissociative mechanism. In both molecules at the η^3 structures the hydrides bridge in an unsymmetrical fashion. A rationale is given for these trends.

The borohydride ligand can bond to a transition metal in an η^3, η^2 or η^1 manner (**1–3**), respectively. Examples of each coordination type are known and have been structurally categorized.[1] In this way it is like its isolobal partner, the cyclopentadienyl ligand.[2] Most frequently, the borohydride ligand undergoes bridging–terminal hydride exchange. However, not much is known about the reaction mechanism(s) for this process. In particular, for a complex with an η^2 ground state, transition states having η^1 or η^3 coordination, among others, are conceivable.[3] In this work we shall concentrate on the dynamics associated with 18-electron (η^2-$BH_4)ML_4$ and ML_2 species via molecular orbital calculations at the *ab initio* level. Previous theory[4–9] has focused primarily on early transition metal and main group compounds.

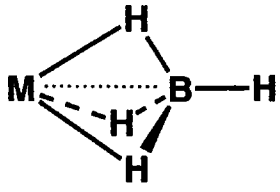

1

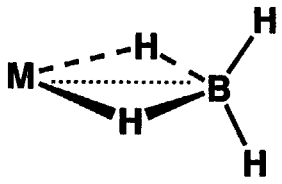

2

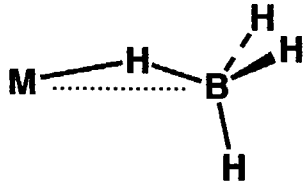

3

One might have expected that electron counting considerations would play an important role in determining the transition state. If an η^2 complex (**2**) possesses 18 electrons around the transition metal, then a dissociative mechanism for bridging–terminal hydride exchange via the η^1 species (**3**) will be at a 16-electron count. Alternatively, an associative transition state at the η^3 geometry (**1**) requires a 20-

*Dedicated to Professor E. W. Abel; a gentleman and a scholar.

†Author to whom correspondence should be addressed.

electron count. A general rule of thumb in organometallic ligand substitution reactions is that dissociative mechanisms (or interchange mechanisms with much dissociative character) are preferred.[10,11] However, the situation is not quite this simple. From a slightly more detailed perspective (*vide infra*) with **2** as the ground state, the metal fragment (M in **2**) must have two empty acceptor orbitals which can interact with two filled B—H σ-bonding orbitals. This stabilizes the two B—H σ-combinations and creates a three-centre–two-electron bonding situation. That is acknowledged by the dotted line between the metal and boron in **2**. Upon going to **3**, one bonding interaction to the metal is lost. Alternatively, in **1** there will be an antibonding interaction between the metal and one B—H σ-bond turned on. The question then is whether the loss of one metal–BH interaction (in **3**) is worth more or less than the introduction of one metal–BH antibonding combination (in **1**). To examine this question we have chosen to use $(BH_4)Mn(CO)_4$ as a model for the isoelectronic and experimentally known[12–14] $(BH_4)Cr(CO)_4^-$, $(BH_4)Mo(CO)_4^-$ and $(BH_4)W(NO)(CO)(PMe_3)_2$ complexes. The model employed for $(BH_4)Cu(PPh_3)_2$[15] was $(BH_4)Cu(PH_3)_2$.

COMPUTATIONAL METHODS

All *ab initio* molecular orbital calculations were carried out using the Gaussian90[16] and GAMESS[17] packages. Effective core potentials with an associated double-zeta basis set for the valence electrons were used for the manganese and copper atoms.[18] The C, O, P and H (for the PH_3 ligands) atoms were kept at the 3-21G level.[19] Special care was taken with the borohydride ligand. Previous work on transition-metal borohydrides showed that relative energies were sensitive to polarization functions on the B and H atoms.[20] The geometry optimizations used a 3-21G basis set for B and H.[19] Single point calculations using a 6-31G** basis[21] were used where *p* and *d* functions have been added to H and B, respectively. Additionally, since the BH_4 ligand remains somewhat anionic, single point calculations were also carried out with a 6-31++G** basis,[22] where extra diffuse *s* and *sp* shells were added to H and B, respectively. The collected basis sets will be referred to as 3-21G, 6-31G** and 6-31++G**. Geometry optimization for each of the structures employed the 3-21G basis at the Hartree–Fock (HF) level. Listings of the Cartesian coordinates for each optimized geometry are available from the authors upon request. The effects of electron correlation on the relative stability were tested by second-order Møller–Plesset perturbation theory (MP2) using the frozen core approximation. Extended Hückel calculations[23] were carried out using a modified Wolfsberg–Helmholz formula.[24] The H_{ii} and orbital exponents were taken from the literature[23,25,26] and are listed in Table 1.

RESULTS

Geometry optimizations of $(BH_4)Mn(CO)_4$ on the four structures shown in **4**–**7** were carried out using the 3-21G basis at the HF level. The two η^3 isomers **6** and **7** are related by a 30° rotation of the borohydride ligand. Pilot calculations on the 30° rotamer of the η^1 structure showed that it was essentially identical in energy with **5**. C_{2v} symmetry was enforced for the η^2 isomer (**4**) and C_s symmetry for the other three structures. An η^1 transition state having a bent Mn—H—B bond angle could not be located. All attempts simply resulted in a return to the η^2 or η^3 species. Therefore, this bond angle was constrained to be 180° in **5**. For computation convenience, the Mn—B—H_t bond angles in **6** and **7** were also kept linear. No other impositions on the optimizations were enforced. Selected bond distances and angles for **4**–**7** are reported in Table 2. A comparison of the η^2 structure to experiment is also given in Table 2 for $(\eta^2\text{-}BH_4)Cr(CO)_4^-$.[12] This is an X-ray diffraction structure so the position of the hydrogen atoms suffer from systematic errors.[1e,27] In particular the B—H_t distances of 0.90 (7) Å are very short compared with the 1.15–1.23 Å range of values from neutron structures,[28] with

Table 1. Parameters used in the extended Hückel calculations

Orbital		H_{ii} (eV)	ζ_1	ζ_2	c_1[a]	c_2[a]	Ref.
Cu	4*s*	−11.40	2.20				25
	4*p*	−6.06	2.20				
	3*d*	−14.00	5.95	2.30	0.5933	0.5744	
Mn	4*s*	−9.75	1.90				26
	4*p*	−5.89	1.90				
	3*d*	−11.67	5.15	1.90	0.5311	0.6479	
P	3*s*	−18.60	1.60				23
	3*p*	−14.00	1.60				
B	2*s*	−15.20	1.30				23
	2*p*	−8.50	1.30				
C	2*s*	−21.40	1.625				23
	2*p*	−11.40	1.625				
O	2*s*	−32.30	2.275				23
	2*p*	−14.80	2.275				
H	1*s*	−13.60	1.30				23

[a] Contraction coefficient for the double zeta expansion.

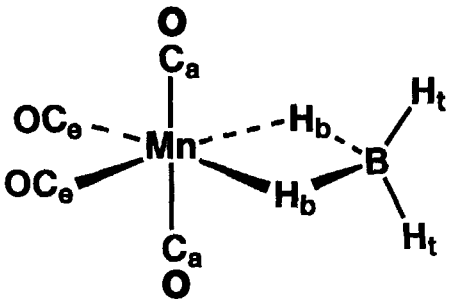

4

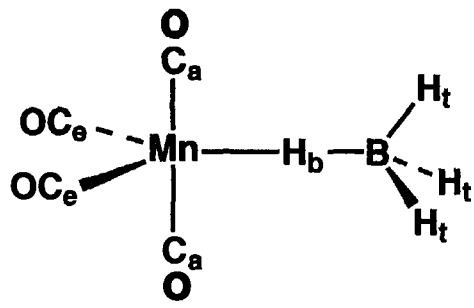

5

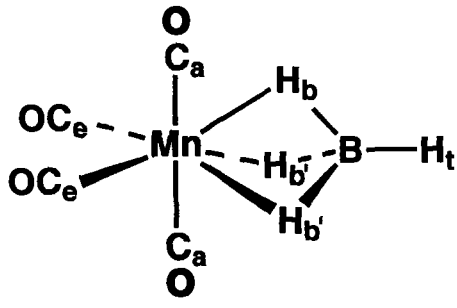

6

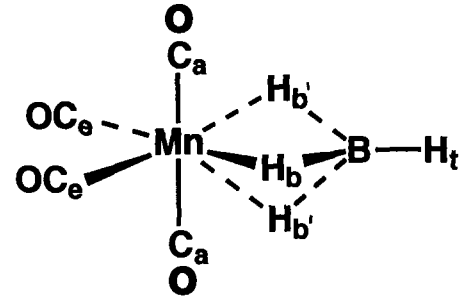

7

Table 2. Selected bond distances (Å) and angles (°) in $(BH_4)Mn(CO)_4$

	exp[a]	4	5	6	7
Mn—B	2.29(1)	2.33	3.10	2.40	2.42
Mn—H_b	1.88(7)[b]	1.89	1.81	2.48	2.13
Mn—$H_{b'}$				2.17	2.38
B—H_b	1.13(8)[b]	1.29	1.30	1.23	1.27
B—$H_{b'}$				1.26	1.23
B—H_t	0.90(7)[b]	1.20	1.27[b]	1.20	1.20
Mn—C_a	1.86(1)[b]	2.17	2.09	2.23[b]	2.23
Mn—C_e	1.82(1)[b]	2.13	2.16	2.14	2.14[b]
Mn—H_b—B	98(4)[b]	92.7	180.0	71.8	86.9
Mn—$H_{b'}$—B				84.3	73.2
B—Mn—C_a	92.2(4)[b]	85.4	84.6[b]	88.1[b]	87.9
B—Mn—C_e	132.6(4)[b]	131.9	132.3	131.9	132.0[b]
C_e—Mn—C_e	94.8(4)	96.2	94.5	96.2	96.1

[a] For $(\eta^2\text{-}BH_4)Cr(CO)_4^-$.[12]
[b] Averaged values.

most distances lying near 1.19 Å. Likewise, the B—H_b distances are in the 1.25–1.29 Å range[28] rather than the X-ray value of 1.13 (8) Å. The optimized values for **4** are in close agreement to the neutron results. There is also close agreement between the experimental and theoretical bond angles. The calculations do have a serious error in that the Mn—C distances are approximately 0.3 Å too long. This is in fact a typical result for metal–carbonyl bond lengths at the HF level.[29] The error

Table 3. Selected bond distances (Å) and angles (°) in $(BH_4)Cu(PH_3)_2$

	exp[a]	8	9	10	11
Cu—B	2.184(9)	2.31	2.96	2.22	2.22
Cu—H_b	2.02(5)	1.89	1.66	2.11	2.16
Cu—$H_{b'}$				2.15	2.12
B—H_b	1.26(4)	1.27	1.31	1.25	1.24
B—$H_{b'}$				1.25	1.25
B—H_t	1.37(5)	1.21	1.21[b]	1.20	1.20
Cu—P	2.276(1)	2.58	2.56	2.60	2.60[b]
Cu—H_b—B	80(5)	91.8	180.0	78.1	76.2
Cu—$H_{b'}$—B				76.5	77.7
P—Cu—P	123.26(6)	122.6	131.8	120.6	124.4

[a] For $(\eta^2\text{-}BH_4)Cu(PPh_3)_2$.[15]
[b] Averaged values.

persists in structures **5**–**7**, therefore, this feature should not create a bias in the relative energies.

Table 3 gives the structural features associated with $(BH_4)Cu(PH_3)_2$. Just as in the Mn complex, C_{2v} symmetry was used for the η^2 complex (**8**) along with C_s symmetry for the η^1 (**9**) and two η^3 structures (**10** and **11**). The Cu—H_b—B bond angle in **9** and the Cu—B—H_t angles in **10** and **11** were again constrained to be linear. Table 3 compares the optimized η^2 structure (**8**) with the X-ray structure for $(\eta^2\text{-}BH_4)Cu(PPh_3)_2$.[15] In this case the experimental value for the B—H_t distance appears to be long. The computed value of 1.20 Å lies within the range of neutron structure values cited previously. The computed Cu—P distances are *ca* 0.3 Å too long in all structures. The agreement between experiment and theory is good for the remaining distances and angles. Notice that the Cu—H bond length at 1.66

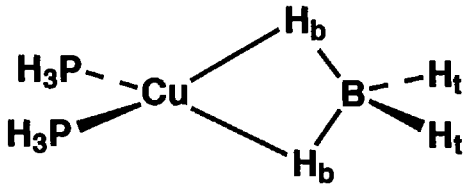

8

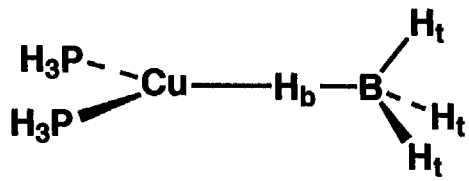

9

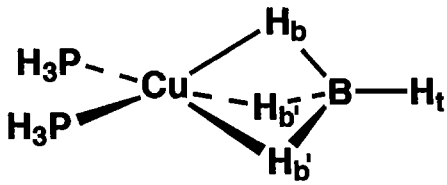

10

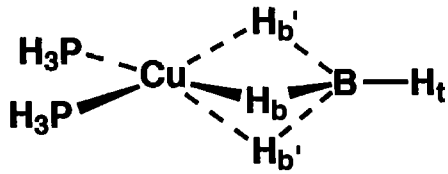

11

Å for the η^1 geometry (**9**) is predicted to be considerably shorter than that for the η^2 isomer. It is interesting to note that in the neutron structure[30] for $(\eta^1\text{-}BH_4)Cu(PPh_2Me)_2$ the Cu—H_b distance is 1.697 (5) Å which is in good agreement with our calculated value for **9**. In $(\eta^1\text{-}BH_4)Cu(PPh_2Me)_2$ the Cu—H_b—B angle is 121.7 (4)°, not the 180° we have fixed in **9**. Bo and Dedieu[9] have reported that at the HF *ab initio* level it requires only 1.4 kcal mol^{-1} in $(\eta^1\text{-}BH_4)Cu(PH_3)_3$ to bend the Cu—H_b—B bond angle from the experimental value to a linear one. We suspect the same would be true in **9** (and in **5**). It should be noted that there is considerable asymmetry in the η^3 bonding modes for **6**, **7**, **10** and **11**. This is more evident in the metal–H_b distances than for the other structural parameters. We shall return to this anomaly in the next section of this paper.

The computed energies (kcal mol^{-1}) relative to the η^2 structure for **5**–**7** and **9**–**11** are given in Table 4. In both compounds the η^2 isomer (**4** and **8**) were found to be at the lowest energy. Also listed are the calculated total energies for **4** and **8**. It is clear from the data that the relative energies change only slightly when one goes from one basis set level to another. In each system the inclusion of electron correlation by the MP2 method increases the relative energies but does not change their ordering. The η^1 structure is consistently *ca* 10 kcal mol^{-1} higher in energy than either η^3. Notice that this value is much larger than an estimate of 1–2 kcal mol^{-1} of stabilization associated with allowing the M—H_b—B bond to relax from 180°. The two η^3 geometries are always very close to each other in energy.

Experimentally, bridging–terminal hydride exchange was found to be rapid at −106°C for $(\eta^2\text{-}BH_4)Cu(PPh_3)_2$[31] and even at −165°C for $(\eta^2\text{-}BH_4)Cu[P(OMe)_3]_2$.[32] Our calculated barriers of 3–4 kcal mol^{-1} at the HF level are consistent with this. The MP2 barriers at 7.4 kcal mol^{-1} appear to be too large. This is also most likely to be the case with $(\eta^2\text{-}BH_4)Mn(CO)_4$. Bridging–terminal hydride exchange in $(\eta^2\text{-}BH_4)Cr(CO)_2^-$ was rapid at −80°C[12] and in $(\eta^2\text{-}BH_4)Mo(CO)_4^-$, $\Delta G\dagger$ was measured to be 10.0 ± 0.2 kcal mol^{-1}.[13] The neutral Mn model in our studies is expected to be more covalently bonded to the borohydride ligand than in the previous two molecules, and hence a somewhat higher barrier may be anticipated. We note that there is no bridging–terminal exchange at room temperature in the isoelectronic $(\eta^2\text{-}BH_4)IrH_2[P(Bu\text{-}t)_3]_2$ complex.[33] This is also true even at 33°C for $(\eta^2\text{-}BH_4)FeH(tppme)$[34] where tppme = $MeC(CH_2PPh_2)_3$; the barrier must be quite a bit higher than 10 kcal mol^{-1}. An associative process via an η^3-BH_4 ligand has been experimental established[3] for $CpCp^*Ta(\eta^2\text{-}BH_4)$. It is also the mechanism favoured by Darensbourg, Marks and coworkers[12,13] for $(\eta^2\text{-}BH_4)Cr(CO)_4^-$ and $(\eta^2\text{-}BH_4)Mo(CO)_4^-$ since one might expect carbonyl site exchange in a 16 electron, five coordinate species where the borohydride ligand is bound in an η^1 fashion. No carbonyl exchange was found even at elevated temperatures. We shall return to this point in the next section. Our theoretical results decidedly point to an associative (η^3) process for bridging–terminal hydride exchange in 18-electron $(\eta^2\text{-}BH_4)ML_4$ and ML_2 complexes. This is contrary to the electron counting arguments given in the Introduction. We now proceed to establish why this can be this case.

Table 4. Calculated relative energies (kcal mol^{-1})

$(BH_4)Mn(CO)_4$	**5**	**6**	**7**	E_{TOT}[a]
HF/3-21G	24.3	14.4	14.9	−490.22266
HF/6-31G**	26.9	15.6	16.2	−490.38124
HF/6-31++G**	28.0	16.9	17.8	−490.38990
MP2/6-31G**	40.1	25.9	27.9	−491.53540
$(BH_4)Cu(PH_3)_2$	**9**	**10**	**11**	E_{TOT}[a]
HF/3-21G	12.0	3.3	3.0	−758.71644
HF/6-31G**	13.9	3.7	3.4	−758.87363
MP2/6-31G**	20.3	7.4	7.4	−759.33765

[a] Calculated total energies (hartrees) for the η^2 isomer.

DISCUSSION

A qualitative rationale for bridging–terminal hydride exchange in 18-electron $(BH_4)ML_4$ and ML_2 complexes can be constructed in the following manner. Consider $(\eta^2\text{-}BH_4)Mn(CO)_4$ (**4**). An orbital interaction diagram for this complex is shown on the left side of Fig. 1. Three important valence orbitals of a C_{2v} $Mn(CO)_4^+$ fragment[35] are explicitly drawn. The a_1 and b_2 fragment orbitals are the two lowest empty ones and they interact strongly with two filled BH_4^- σ-bonding orbitals, $2a_1$ and b_2. In reality, a_1 on $Mn(CO)_4^+$ does also stabilize $1a_1$, the lowest orbital of BH_4^-. The formation of two-electron–three-centre bonding is clear. Electron density from especially the filled b_2 and $2a_1$ orbitals which are strongly B—H σ-bonding occurs to the two empty hybrids on $Mn(CO)_4^+$. This should cause the bridging B—H bonds to become weakened. This is also clear from the *ab initio* calculations. The B—H_b distances for

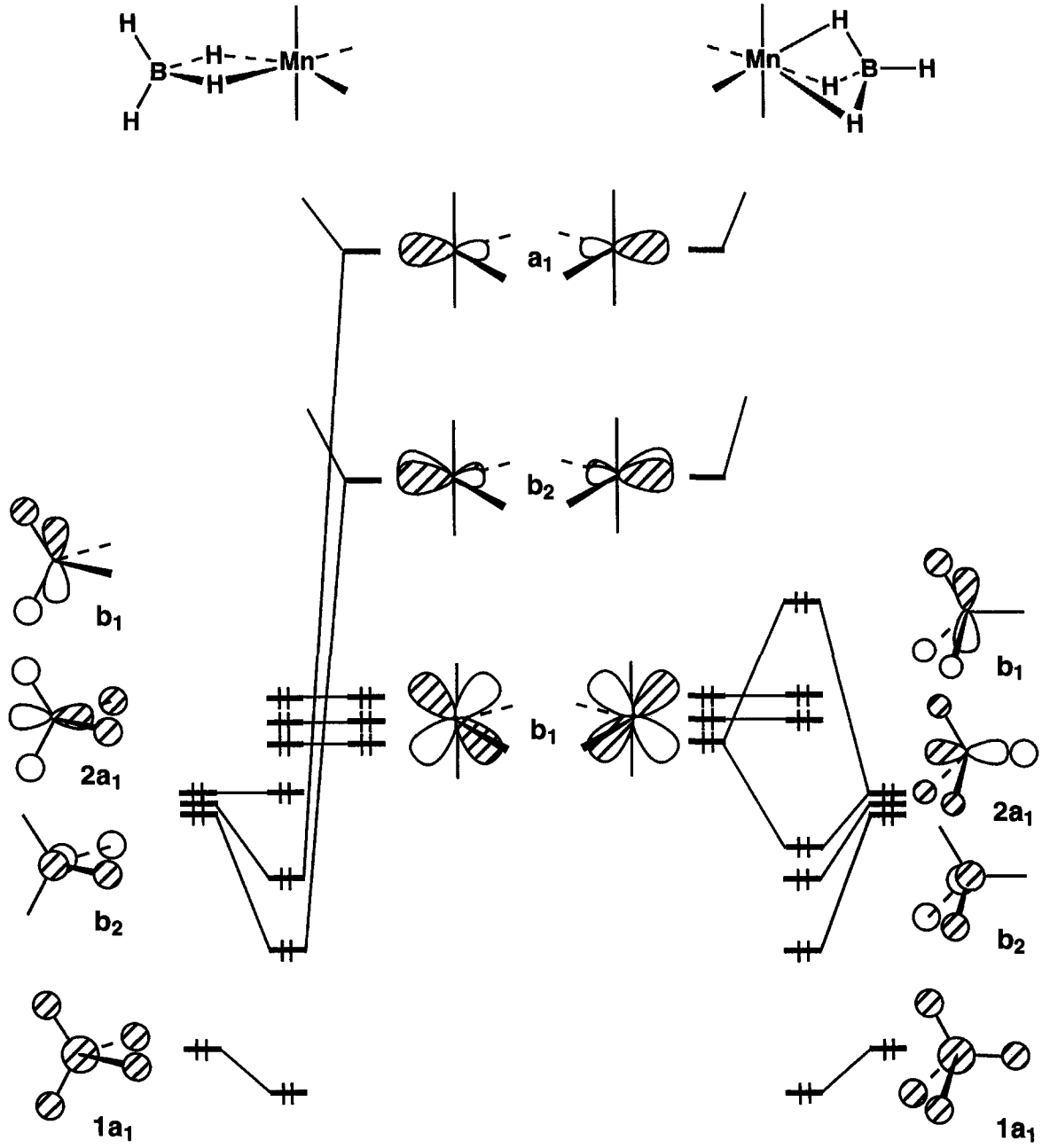

Fig. 1. An orbital interaction diagram for $(\eta^2\text{-}BH_4)Mn(CO)_4$ (left) and $(\eta^3\text{-}BH_4)Mn(CO)_4$ (right).

all four isomers are longer than the B—H_t ones (see Table 2). On going to the η^1 geometry (**5**) the interaction of $Mn(CO)_4^+$ a_1 with $1a_1$ and $2a_1$ (see the right side of Fig. 1 for the appropriate combination of BH_4^- orbitals) remains very strong. However, interaction between the b_2 fragments is all but lost. The Mn—B distance is quite long at this geometry. On the other hand, that interaction can be retained at the η^3 structure. An interaction diagram for the geometry given by **6** is presented on the right side of Fig. 1. The price to be paid is that here the filled b_1 orbital on $Mn(CO)_4^+$ overlaps with the occupied b_1 BH_4^- fragment orbital; at η^2 it was non-bonding. The result is a net four-electron–two-orbital repulsion, which importantly is a function of the overlap between the two fragment orbitals.[35] The same situation will apply when the BH_4 ligand is rotated to **7**; the b_1 and b_2 functions simply interchange their roles. It this context it is also easy to see why there is so little calculated energy difference between **6** and **7**; see Table 4.

As mentioned in the Introduction, there is then a balance between how much energy is lost when b_2 on BH_2^- remains non-bonding at η^1, compared

Table 5. Overlap integrals between the ML_n and BH_4 fragments

$(BH_4)Mn(CO)_4$	**4**	**5**	**6**
$\langle a_1 \mid 2a_1 \rangle$	0.265	0.239	0.265
$\langle a_1 \mid 1a_1 \rangle$	0.259	0.131	0.228
$(BH_4)Cu(PH_3)_2$	**8**	**9**	**10**
$\langle a_1 \mid 2a_1 \rangle$	0.308	0.308	0.335
$\langle a_1 \mid 1a_1 \rangle$	0.259	0.148	0.265

with the net antibonding between the b_1 fragment orbitals at η^3. It would appear from our calculations that the latter is energetically less costly, but there are two other considerations which favour an η^3 process. First of all, the interaction between the a_1 hybrid on $Mn(CO)_4^+$ and the $2a_1$ along with the $1a_1$ BH_4^- fragment orbitals are not equal in their η^1 and η^3 geometries. At η^1 the interaction to the metal is via one hydrogen atom, whereas at η^3 it is to three hydrogens and the boron atom.[36] There is, of course, a geometry change in that the Mn—H_b distance is much shorter at the η^1 structure compared with those at the η^3 geometry, see Table 2. To investigate this factor we carried out extended Hückel calculations for **4**–**6** at the geometries obtained from the HF calculations. The relevant overlap integrals are presented in Table 5. The important point is that they are larger at the η^3 geometry (**6**) than they are at η^1 (**5**). This means that the $2a_1$ and $1a_1$ orbitals of BH_4^- are stablized to a greater extent in **6** compared with **5**. Secondly, the Mn—H_b bonds are significantly longer in the two η^3 structures. This is primarily due to the antibonding between the b_1 fragment orbitals which is turned on at these geometries. Increasing the Mn—H_b distance decreases the overlap and, therefore, decreases the net repulsion between these orbitals. However, there is more detail here. As previously mentioned, there are two different distances to the bridging hydrogen atoms, Mn—H_b and Mn—$H_{b'}$ see Table

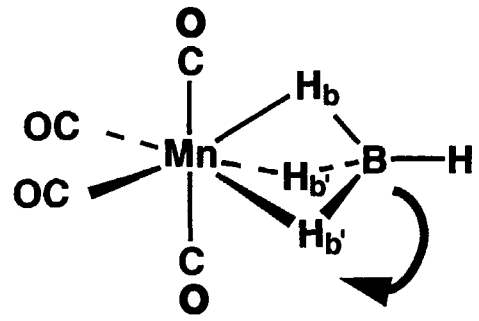

12

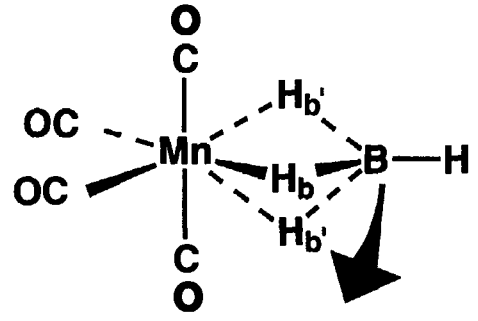

13

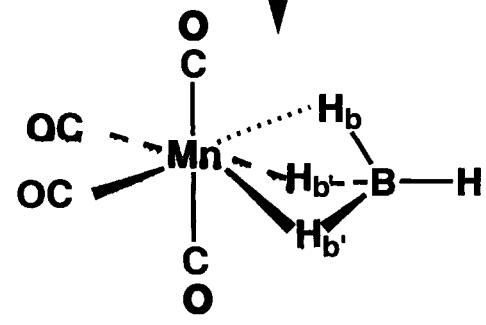

14

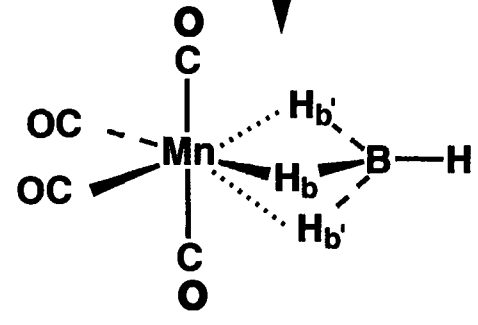

15

2. What occurs in **6** is a rocking motion, shown in **12**, which causes the Mn—$H_{b'}$ distances to be longer than Mn—H_b. For **7** the rocking motion occurs out of the plane of the paper (**13**). Now the Mn—$H_{b'}$ distances are longer than Mn—H_b. Both deformations reduce the overlap and antibonding between the b_1 orbitals while keeping that between the a_1 and b_2 fragment orbitals strong. The Mn—H_b bonding in **14** and Mn—$H_{b'}$ bonding in **15** is considerably weakened. One might regard them as being agostic bonds. It is interesting that a Mo–ethyl species akin to **15** has been proposed as an intermediate.[37] As previously mentioned, there is good experimental evidence that no carbonyl exchange occurs in this dynamic process.[12,13] If an η^1 species were involved as an intermediate, then there is ample theoretical and experimental precedent that the structure should be based on a square pyramid and that rapid axial–basal exchange would take place which equivalences the carbonyl groups.[38] It is unclear whether this would be the case for an η^1 transition state. However, notice that in **15**, H_b and the four carbonyls define a square pyramid. Relaxation of the borohydride to bring the two $H_{b'}$ atoms into an agostic bonding distance to the vacant coordination site will be stabilizing and this will then block an apical–basal exchange. The definition of η^3 and η^1 coordination becomes blurred.

The situation for $(BH_4)Cu(PH_3)_2$ is very similar to that just presented with one important difference. An idealized orbital interaction diagram for $(\eta^2\text{-}BH_4)Cu(PH_3)_2$ is presented on the left side of Fig. 2. The orientation of the BH_4^- ligand is rotated by 90° relative to that in Fig. 1. This is a d^{10} complex, so in the important valence orbitals of the ML_2 unit the b_2 orbital is occupied and a_1 is the lowest unoccupied orbital.[35] The interaction of a_1 to the $2a_1$ and $1a_1$ fragment orbitals of BH_4^- is identical to that presented before. There are now two orbitals of b_1 symmetry at the metal which need to be considered, $1b_1$ and $2b_1$. Due to the BH_4^- orientation, b_1 at BH_4^- and $1b_1$ along with $2b_1$ on $Cu(PH_3)_2^+$

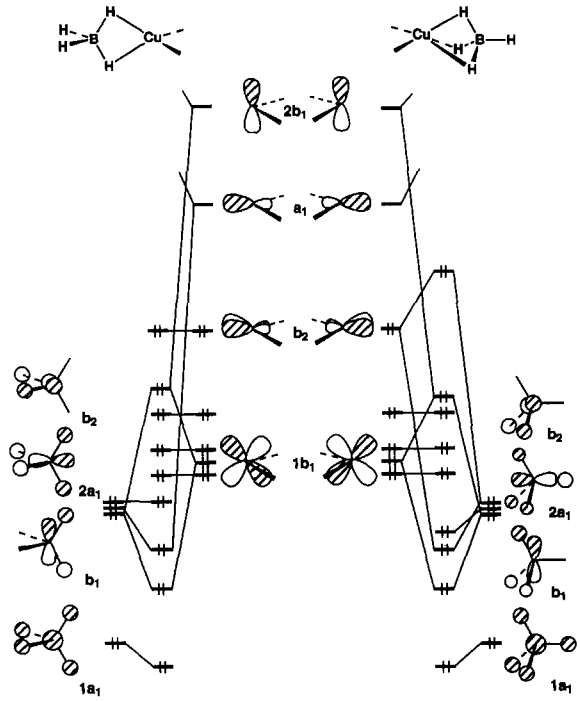

Fig. 2. An orbital interaction diagram for $(\eta^2\text{-}BH_4)Cu(PH_3)_2$ (left) and $(\eta^3\text{-}BH_4)Cu(PH_3)_2$ (right).

now interact at the η^2 geometry. A typical three-orbital pattern evolves With four electrons in the b_1 set, this is a net bonding situation. The middle molecular level along with the non-bonding b_2 form two out of the three members of the "t_2" set in this psuedo-tetrahedral complex. At the η^3 geometry (the right side of Fig. 2). The b_2 fragment orbital on $Cu(PH_3)_2^+$ now does interact strongly with b_2 on BH_4^-. Both orbitals are filled and a net antibonding situation is created. However, like $(BH_4)Mn(CO)_4$ there are two factors which favour η^3 coordination over η^1. As demonstrated in Table 5, the overlap between the a_1 fragment orbital on $Cu(PH_3)_2^+$ and $2a_1$ along with $1a_1$ on BH_4^- is larger at η^3 than it is at η^1. Secondly, there is a geometrical distortion away from a "perfect" η^3 geometry. In

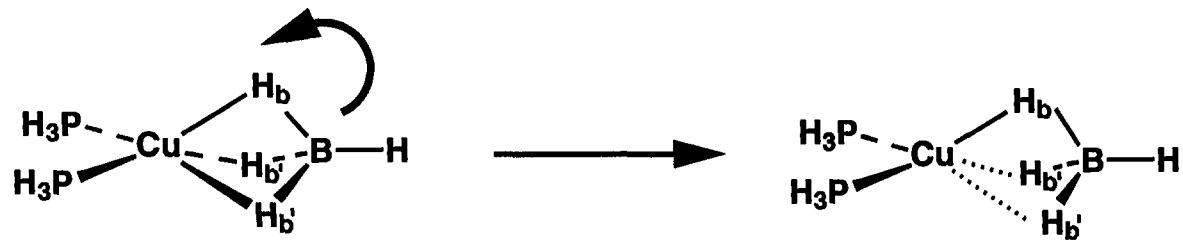

10 **16**

particular, the BH_2^- ligand in **10** rocks in the opposite sense as that given by **12** to yield **16**. This decreases the repulsion between the two b_2 orbitals. A 16-electron $(\eta^1\text{-}BH_4)Cu(PH_3)_2$ complex should be stable at a trigonal planar geometry.[35] However, it is also clear that the empty $2b_1$ fragment orbital on $Cu(PH_3)_2$ at the middle of Fig. 2 can be used to stabilize two "agostic" bonds on the borohydride ligand by distorting to **16**. Referring back to Table 3, one can see that this distortion is not as strong as that found for $(\eta^3\text{-}BH_4)Mn(CO)_4$, nevertheless, we believe that the distortion is not an artifact of the computational technique.

CONCLUSIONS

Structural details around the metal–borohydride region of the molecules are in good agreement with experiment at the HF level. We have not computed the vibrational frequencies associated with the optimized geometries for these structures. Nor has the reaction path been followed by an intrinsic reaction coordinate method. However, the *ab initio* calculations show that η^2 geometries in both compounds are more stable than any other alternative, in agreement with experiment. Furthermore, η^3 structures are decisively more stable than linear η^1 alternatives at all computational levels. We propose that the fluxionality in $(BH_4)Mn(CO)_4$ occurs via **15**, where two of the three bridging hydrides are bound to Mn in a considerably weaker fashion than the third. In $(BH_4)Cu(PH_3)_2$ we feel that the transition state resembles **16** with again two Cu—H bonds weaker than the third. It is clear that the calculations at the MP2 level do overestimate the barrier in both instances.

Acknowledgements—We thank the Robert A. Welch Foundation and the donors of the Petroleum Research Fund as administered by the American Chemical Society for support of this work and the National Science Foundation for a generous allocation of time at the Pittsburgh Supercomputing Center. Y. O. thanks the Rotary Foundation for making his stay at Houston possible.

REFERENCES

1. For reviews, see (a) T. J. Marks and J. R. Kolb, *Chem. Rev.* 1977, **77**, 263; (b) J. D. Kennedy, *Prog. Inorg. Chem.* 1984, **32**, 519; (c) B. D. James and M. G. H. Wallbridge, *Prog. Inorg. Chem.* 1970, **11**, 99; (d) K. G. Gilbert, S. K. Boocock and S. G. Shore, in *Comprehensive Organometallic Chemistry*, edited by G. W. Wilkinson, F. G. A. Stone and E. W. Abel, Vol. 6, p. 879. Pergamon Press, Oxford (1982); (e) R. Bau, R. G. Teller, S. W. Kirtly and T. F. Koetzle, *Acct Chem. Res.* 1979, **12**, 176.
2. (a) M. Mancini, P. Bougeard, R. C. Burns, M. Mlekuz, B. G. Sayer, J. I. A. Thompson and M. J. McGlinchey, *Inorg. Chem.* 1984, **23**, 1072; (b) A. G. Császár, L Hedberg, K. Hedberg, R. C. Burns, A. T. Wen and M. J. McGlinchey, *Inorg. Chem.* 1991, **30**, 1371; (c) A. P. Hichkock, N. Hao, N. H. Werstiuk, M. J. McGlinchey and T. Ziegler, *Inorg. Chem.* 1982, **21**, 793.
3. A complete delineation of the mechanistic types may be found in M. L. H. Green and L.-Y. Wong, *J. Chem. Soc., Dalton Trans.* 1989, 2133.
4. (a) A. Lledos, M. Duran, Y. Jean and F. Volatron, *Inorg. Chem.* 1991, **30**, 4440; (b) F. Volatron, M. Duran, A. Lledos and Y. Jean, *Inorg. Chem.* 1993, **32**, 951; (c) A. Jarid, A. Lledos, Y. Jean and F. Volatron, *Inorg. Chem.* 1993, **32**, 4695; (d) A. Lledos, M. Duran, Y. Jean and F. Volatron, *Bull. Soc. Chim. Fr.* 1992, **129**, 216.
5. (a) R. Bonaccorsi, O. P. Charkin and J. Tomasi, *Inorg. Chem.* 1991, **30**, 2964; (b) D. G. Musaev and O. P. Charkin, *Zh. Neorg. Khim.* 1991, **36**, 760; (c) A. S. Zyubin, M. Kaupp, O. P. Charkin and P. v. R. Schleyer, *Zh. Neorg. Khim.* 1993, **38**, 1387 and refs therein.
6. D. Hohl and N. Rösch, *Inorg. Chem.* 1986, **25**, 2711.
7. J. W. Lauher and R. Hoffmann, *J. Am. Chem. Soc.* 1976, **98**, 1729.
8. C. J. Dain, A. J. Downs, M. J. Goode, D. G. Evans, K. T. Nicholls, D. W. H. Rankin and H. E. Robertson, *J. Chem. Soc., Dalton Trans.* 1991, 961.
9. C. Bo and A. Dedieu, *Inorg. Chem.* 1989, **28**, 304.
10. J. D. Atwood, *Inorganic and Organometallic Reaction Mechanisms*, pp. 103–156. Brooks/Cole, Monterey, CA (1985).
11. S.-K. Kang, T. A. Albright and C. Mealli, *Inorg. Chem.* 1987, **26**, 3158.
12. M. Y. Darensbourg, R. Bau, M. W. Marks, R. R. Burch, Jr., J. C. Deaton and S. Slater, *J. Am. Chem. Soc.* 1982, **104**, 6961.
13. S. W. Kirtly, M. A. Andrews, R. Bau, G. W. Grynkewich, T. J. Marks, D. L. Tipton and B. R. Whittlesey, *J. Am. Chem. Soc.* 1977, **99**, 7154.
14. A. A. H. van der Zeijden, V. Shklover and H. Berke, *Inorg. Chem.* 1991, **30**, 4393.
15. S. J. Lippard and K. M. Melmed, *Inorg. Chem.* 1967, **6**, 2223.
16. M. J. Frisch, M. Head-Gordon, J. B. Foresman, G. W. Trucks, H. B. Schlegel, K. Raghavachari, M. A. Robb, J. S. Binkley, C. Gonzalez, D. J. Defrees, D. J. Fox, R. A. Whiteside, R. Seeger, C. F. Melius, J. Baker, L. R. Kahn, J. J. P. Stewart, E. M. Fluder, S. Topiol and J. A. Pople, Gaussian90. Gaussian, Inc., Pittsburgh, PA (1990).
17. M. W. Schmidt, K. K. Baldridge, J. A. Boatz, J. H. Jensen, S. Koeski, M. S. Gordon, K. A. Nguyen, T. L. Windus and S. T. Elbert, *QCPE Bull.* 1990, **10**, 52.
18. P. J. Hay and W. R. Wadt, *J. Chem. Phys.* 1985, **82**, 299.
19. J. S. Binkley, J. A. Pople and W. J. Hehre, *J. Am. Chem. Soc.* 1980, **102**, 939; M. S. Gordon, J. S.

Binkley, J. A. Pople, W. J. Pietro and W. J. Hehre, *J. Am. Chem. Soc.* 1982, **104**, 2797.
20. S.-K. Kang and T. A. Albright, unpublished work.
21. J. S. Binkley and J. A. Pople, *J. Chem. Phys.* 1977, **66**, 879.
22. T. Clark, J. Chandrasekhar, G. W. Spitznagel and P. v. R. Schleyer, *J. Comp. Chem.* 1983, **4**, 294.
23. R. Hoffmann and W. N. Lipscomb, *J. Chem. Phys.* 1962, **36**, 2179, 3489; 1962, **37**, 2872; R. Hoffmann, *J. Chem. Phys.* 1963, **39**, 1397.
24. J. H. Ammeter, H.-B. Bügi, J. C. Thibeault and R. Hoffmann, *J. Am. Chem. Soc.* 1978, **100**, 3686.
25. P. J. Hay, J. C. Thibeault and R. Hoffmann, *J. Am. Chem. Soc.* 1975, **97**, 4884.
26. M. Elian and R. Hoffmann, *Inorg. Chem.* 1975, **14**, 1058.
27. R. G. Teller and R. Bau, *Struct. Bonding (Berlin)* 1981, **44**, 1.
28. R. W. Broach, I. Chuang, T. J. Marks, and J. M. Williams, *Inorg. Chem.* 1983, **22**, 1081.
29. (a) A. Veillard, *Chem. Rev.* 1991, **91**, 743; (b) A. Ricca, C. W. Bauschlicher Jr and M. Rosi, *J. Phys. Chem.* 1994, **98**, 9498.
30. F. Takusagawa, A. Fumagalli, T. F. Koetzle, S. G. Shore, T. Schmitkons, A. V. Fratini, K. W. Morse, C. Wei and R. Bau, *J. Am. Chem. Soc.* 1981, **103**, 5165.
31. C. H. Bushweller, H. Beall, M. Grace, W. J. Dewkett and H. S. Bilofsky, *J. Am. Chem. Soc.* 1971, **93**, 2145.
32. J. C. Bommer and K. W. Morse, *Inorg. Chem.* 1978, **17**, 3708.
33. H. D. Empsall, E. M. Hyde, E. Mentzer, B. L. Shaw, and M. F. Uttley, *J. Chem. Soc., Dalton Trans.* 1976, 2069.
34. C. A. Ghilardi, P. Innocenti, S. Midollini and A. Orlandini, *J. Chem. Soc., Dalton Trans.* 1985, 605.
35. T. A. Albright, J. K. Burdett and M.-H. Whangbo, *Orbital Interactions in Chemistry*. John Wiley, New York (1985).
36. Notice from Tables 2 and 3 that the M—B distance does not change much on going from η^2 to η^3. This is consistent with experimental results.[28,30] The long M—B distances for the η^1 structures are a consequence of enforcing linear M—H_b—B bond angles.
37. M. L. H. Green and L.-L. Wong, *J. Chem. Soc., Chem. Commun.* 1989, 677.
38. T. A. Albright, J. K. Burdett and M.-H. Whangbo, *Orbital Interactions in Chemistry*, pp. 313–320 and refs therein. John Wiley, New York (1985).